Obtaining and Analysis of Different Powders to be Used as Modifying Agents in Formation of Polymers with Special Properties

MARIUS BODOR[1,2], IULIA GRAUR[1,2], VASILE BRIA[1], ALINA CANTARAGIU[1], ADRIAN CIRCIUMARU[1,2]*

[1] Dunarea de Jos University of Galati, Research and Development Center for Thermoset Matrix Composites, 47 Domneasca Str., 800201, Galati. Romania

[2] Diagnose and Measurements Group, 41 Rosiori Str., 800055, Galati, Romania

The obtaining of polymers with special properties is dependent on both conditions and materials used in the formation process. This work presents the obtaining, by using the sol-gel method (and citric acid used as in mixture fuel), of some powdery materials destined to be used as additives in polymers' formation. Different types of salts were used in the powders' obtaining process, the long term purpose being to add special properties to polymeric materials, such as good electrical conductivity or photovoltaic capabilities. The materials and methods are thoroughly presented, proving the obtaining repeatability of these powders. Different characterization techniques were used and presented in this paper, from Scanning Electron Microscopy (SEM) for morphology, to EDX for elemental composition, Raman scattering for vibrational properties, thermal analysis by differential scanning calorimetry (DSC), and electrical resistivity for electrical conductivity calculation.

Keywords: modifying agents, powders characterization, special properties polymers

Sometimes, special properties are needed for polymeric materials, depending on the purpose of their utilization. The obtaining of this kind of materials is possible by different additives that may be used, in the form of nanotubes **[1]**, fibers **[2]** or powders with various dimensions [3-7]. The utilization of powders as additives in polymeric resigns has become a common practice in obtaining materials used for different purposes, as for example: polymer light-emitting devices [8, 9], polymer electrolyte membranes for fuel cell applications [10, 11], water filtration membranes [12, 13], etc.

The materials synthesized (by using the sol-gel method) and then analyzed in the present study are of powdery state, the sol-gel method being a cost-effective and easily reproducible process. More importantly, this method has the distinct advantage in excellent composition control, and the ability to achieve atomic scale mixing of individual components [14, 15]. Also, the sol-gel method is known to be a simple process that can be used in obtaining nanopowders of high purity and controlled morphology [16]. In the case of this study, citric acid was also used in the powders formation process, this acid being known as a chelating agent [17] and as a fuel for the reactions that take place in the mixture [18]. This process of utilizing citric acid as fuel for the mixture, and alcohols in order to dissolve the necessary salts, is also known as the citrate gel (Pechini) method [19]. The formation of complex nanopowders by sol-gel method, already approached by other research groups, was sometimes followed by thoroughly made analyzes [20-23]. The purpose of the present paper was to present that the main goals were fulfilled, namely the obtaining of nano-sized particles powder with a high electrical conductivity, both considered necessary in the future applications of these materials. Thus, only the most representative analyzing procedures were presented in this work, starting with morphology and elemental composition realized by SEM-EDX technology, continuing with a glimpse on the vibrational properties using the Raman Scattering, thermal analysis by DSC and finally the calculation of electrical conductivity based on electrical resistivity measurements.

Experimental part

Materials and methods

Reaching the purpose of this research was made possible by using different kind of materials obtained from Sigma Aldrich. Also, the analyzing methods were carried out using multiple apparatuses with characteristics presented below.

From three to four salts were used for each synthesized powdery material and also, every powder was obtained by using the same stirring and quenching times and temperatures. All these and the quantity of the obtained material are presented in table 1. Also, table 1 presents the notation given for each synthesized material which, due to uncertainties on the mineralogical composition, does not depict the exact expected chemical formulas.

The salts presented in table 1 were purchased by Sigma-Aldrich while the ethanol and the citric acid are commercially available.

The obtaining of the additives was possible by using two similar sol-gel methods. The first method consisted in mixing the salts separately with the appropriate amounts of Ethanol and Citric acid, until the formation of a gel-like substance. The substances were then mixed together for 24 hours at 60°C (using a SCILOGEX, MS-H280-Pro type mixer/heater), the resulted gel being quenched for 6 h at 800°C using a LMH 07/12 type furnace (produced by LAC). After quenching, a powder was obtained then milled by using a mortar and a pestle, than analyzed by different methods hereinafter described.

The second obtaining method consisted in mixing all salts together with the Ethanol and the Citric acid and all the other steps were identical with the first method. Considering that the results were similar for each method, the second one will be used in our further researches, taking

* *email: adrian.circiumaru@ugal.ro; Tel.: 00407730290022*

Powder notation/quantity obtained [g]	Materials and their fraction used to obtain the powder	Stirring time/temperature [h/°C]	Quenching time/temperature [h/°C]
$Bi_{x1}Ba_{x2}Sn_{x3}Li_{x4}O_{x5}$ /36.73	$Bi_5H_9N_4O_{22}$ (2M) – 153.88 g $Ba(NO_3)_2$ (2M) – 27.5 g $SnCl_4$ (1M) – 18.45 g LiOH (1M) – 2.208 g Ethanol (95%) – 200 mL Citric acid – 24.92 g	~24/~60	6/800
$Sn_{x1}Bi_{x2}Ni_{x3}O_{x4}$ /63.93	$SnCl_4 \cdot 5H_2O$ (2M) – 73 g $Bi(NO_3)_3 \cdot 5H_2O$ (1M) – 55.5 g $Ni(NO_3)_2 \cdot 6H_2O$ (3M) – 90.87 g Ethanol (95%) – 300 mL Citric acid – 38.43 g		
$Os_{x1}Zr_{x2}Ba_{x3}Ca_{x4}O_{x5}$ /31.91	$OsCl_4$ (0.01 M) – 0.12 g ZrCl (1M) – 7.92 g $BaCl_2$ (3M) – 24.9 g $CaSO_4$ (2M) – 9.51 g Ethanol (96%) – 400 mL Citric acid – 48÷60 g		
$Y_{x1}Ta_{x2}Ba_{x3}Ca_{x4}O_{x5}$ /29.41	YCl_3 (1M) – 7.79 g $TaCl_5$ (1M) – 10.32 g $BaCl_2$ (3M) – 29.31 g $CaSO_4$ (2M) – 10.88 g Ethanol (96%) – 400 mL Citric acid – 48÷60 g		

Table 1
MATERIALS AND STEPS USED TO OBTAIN THE POWDERY ADDITIVES

into account its increased efficiency. Also, it has to be mentioned that the analyses results presented in this paper are those of the materials obtained using the second methodology.

Morphological and EDX analysis methods

The resulted materials were firstly studied from the morphological point of view. This was realized by using the scanning electron microscopy methodology. The analyzed powders were placed on a sample holder using a carbon tape, to decrease the sample mobility. To increase the conductivity, the samples were coated with a 2 nm thick layer of gold using a SPI-Sputter Coater with Etch Mode (West Chester, Pennsylvania, USA) for 40 s, with a current of 18 mA. The apparatus used for these analyses was a Scanning Electron Microscope (SEM) Quanta 200 FEI, operating at 15 kV and with an electron beam current of 110 μA using a second electron detector. The samples were analyzed using magnifications between 50 and 50,000X, the most representative images being presented in the present paper.

The same samples were used for elemental analyses, by using the Energy Dispersive X-ray Microanalysis (EDX) integrated system, attached to the SEM instrument. The EDX had 5 detectors of secondary and backscattered electrons and 1 detector for transmitted electrons. The software utilized for data processing was also used for quantification of chemical composition using ZAF (Z – atomic number, A – absorption, F – fluorescence) correction algorithm, multipoint chemical analysis with matrix effects corrections, and the analysis of concentration profile along a defined line.

Raman scattering

Raman scattering was used to determine vibrational properties of the samples. A StellarNet Inc type LASER and spectrometer (795 nm) were used, and for acquisition and interpretation of the results a StellarNet Inc software and a BIO-RAD software/data base were utilized. The milled samples were analyzed by being exposed directly to the LASER radiation (no vials were used).

DSC analyses

To determine the eventual phase transitions that may occur at different temperatures, Differential Scanning Calorimetry (DSC) technique was used. The installation utilized for these analyses was a Mettler Toledo type DSC1, equipped with a FRS5 sensor. The testing method consisted in a heating rate of 20 °C/min, the lower limit and the upper limit temperatures being 30 and 330 °C respectively.

The samples used in DSC analyses were placed in 40 μL crucibles with a pin, and a cap pierced twice with a needle. The crucibles were weighted with an analytical balance (Mettler Toledo, AB204-S/FACT type) without and then with the sample inside, and again after the end of the analysis with the sample inside. Doing so, the calculation of samples loss in mass was made possible.

Determination of conductivity

The powdery materials obtained in this study are intended to be further used as additives in forming polymers with special properties, such as polymers with semiconducting or photovoltaic properties. Thus, after obtaining, these additives were subjected to electrical resistance tests, that helped providing information regarding their electrical conductivity properties. The same test will also be used for the same materials to observe their behavior in different conditions (different temperatures and electromagnetic wavelengths), these results being the aim of another study of this research group.

The setup used consisted in a 5 kV TeraOhmMeter Metrel, MI2077 type, using the two point measuring method. The sample was placed in a plastic tube with known dimensions (length – 219 mm; diameter – 8 mm). The plastic tube was equipped with one copper cap at each end, the measuring electrodes being in contact with these caps during the tests. The sample was pressed inside the tube, so the contact surface with the caps to be as high as possible. The tension applied to the samples had five different values as follow: 643 V; 1283 V; 1903 V; 2543 V and 3166 V. The electrical resistance results were obtained in GΩ, and using the formulas (1-3), the corresponding conductivities for the analyzed materials were obtained in S/m, the final results representing the average of 5 readings afferent to the 5 values of the tension applied to the sample.

$$\sigma = \frac{1}{\rho} \quad (1)$$

$$R = \frac{\rho l}{S} \quad (2)$$

$$\rho = \frac{SR}{l} \quad (3)$$

where:

σ – electrical conductivity [S/m];

ρ – electrical resistivity [Ωm];

R – electrical resistance [GΩ];

l – the length of the plastic tube [mm];

S – the cap surface area in contact with the sample [mm^2].

Results and discussions

Depending on the materials used to obtain the powders that are the focus of this paper, different results were obtained. Taking into consideration the purpose of the powders, the electrical conductivity is the most important factor that has to be evaluated. Nevertheless, all the other tests will contribute to a better understanding of the behavior of the special polymers that will be obtained using these additives. The morphology conferred a preliminary insight into the particle size distribution of the samples, one of the purposes of this process being to obtain powders with nanometer sized particles. The elemental composition of these particles was assessed by EDX.

Chemical composition of the obtained powders is still an unknown, the Raman scattering, whilst a good tool to determine this factor, could not give an answer due to the limited number of spectra in the BIO-RAD data base. Also, a reason for the lack of chemical composition results is the possibly complex composition of the final materials. However, the resulted spectra are presented hereinafter.

As already stated in [24], using the rule of mixtures, some information regarding the amplitude of a property can be given if the properties of the components and their ratios are known. The same rule can be applied for thermal properties which could be calculated for an eventual composite material if data for each containing material would be at hand. DSC results will be valuable for the future applications of the studied materials. This is why alongside the other tests results presented in this paper, these data are of great importance.

The number of produced powders was twelve, and other combinations will be further used, but this study only presents the ones with the highest electrical conductivity values. This test was selected the most important one, due to the desired future utilization of the additives, above mentioned.

Morphological characterization by Scanning Electron Microscopy

Morphological analysis of the powdery materials revealed, to some extent, the expected dimensions of the constituent particles. The friable property was a clear indicator that the agglomerates forming the studied materials were in fact constituted from small particles, starting from several micrometers and going as low as hundreds of nanometers.

Figure 1 presents the morphology of four powders, obtained by using the SEM imaging. All four images show more or less the same particle size distribution. It can be observed that the particles of $Bi_{X1}Ba_{X2}Sn_{X3}Li_{X4}O_{X5}$ powder have sharper edges than all the other ones, while the $Sn_{X1}Bi_{X2}Ni_{X3}O_{X4}$ powder has some acicular formations among the other particles. Since the obtaining process was the same for all studied powders, the difference in morphology is considered to be due to the different interactions between initial salts used in obtaining these materials.

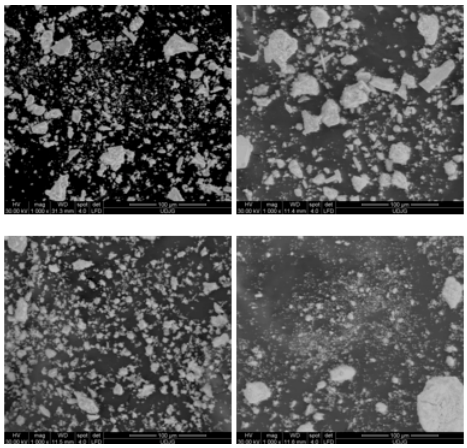

Fig. 1. The morphology of: a – $Bi_{X1}Ba_{X2}Sn_{X3}Li_{X4}O_{X5}$; b – $Sn_{X1}Bi_{X2}Ni_{X3}O_{X4}$; c – $Os_{X1}Zr_{X2}Ba_{X3}Ca_{X4}O_{X5}$ and d – $Y_{X1}Ta_{X2}Ba_{X3}Ca_{X4}O_{X5}$ powders, obtained by using the SEM imaging at 1000X magnification

The same resemblances between samples can be observed in figure 2. These images clearly show that the agglomerates observed in figure 1 are of a brittle constitution, the constituent particles being much smaller, close to nanometer sizes. The particle size distribution of these additives was thus been demonstrated to be in the range of nanometer sizes, clearer results in this regard are to be presented in our future works.

EDX characterization of powders

For all four materials, the results from EDX analysis indicated that the elemental composition is in accordance with the molarity of the chemicals used in the obtaining process. Lithium was an exception due to its very low atomic mass, being unobservable using this analyzing technique.

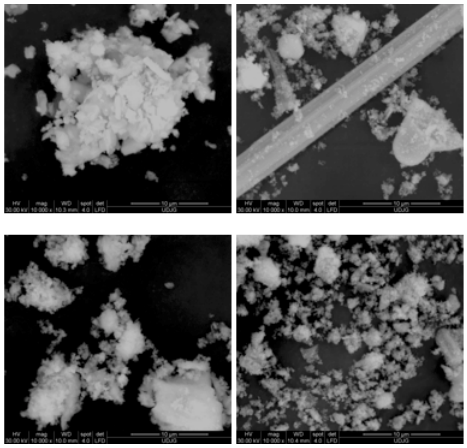

Fig. 2. The morphology of a – $Bi_{X1}Ba_{X2}Sn_{X3}Li_{X4}O_{X5}$, b – $Sn_{X1}Bi_{X2}Ni_{X3}O_{X4}$, c – $Os_{X1}Zr_{X2}Ba_{X3}Ca_{X4}O_{X5}$ and d – $Y_{X1}Ta_{X2}Ba_{X3}Ca_{X4}O_{X5}$ powders, obtained by using the SEM imaging at 10 000X magnification

Table 2

EDX ANALYSIS RESULTS OF $Bi_{X1}Ba_{X2}Sn_{X3}Li_{X4}O_{X5}$ POWDER, FOR ALL THE SURFACE AT 1000X MAGNIFICATION AND IN ONE POINT AT 50 000X MAGNIFICATION

Sample	Elements	Results at 1000X magnification [Wt%]	Results at 50 000X magnification [Wt%]
BiBaSnLi	C	72.23	55.53
	O	10.50	11.21
	Sn	0.89	0.78
	Ba	1.52	2.16
	Bi	14.86	30.32

For numerical results, $Bi_{X1}Ba_{X2}Sn_{X3}Li_{X4}O_{X5}$ powder was selected as an example. Table 2 presents these results, obtained in two different conditions. The first one is the result of scanning the whole surface at 1000X magnification while the second one is the result of point analysis made on a grain at 50,000X magnification. The element gold was ruled out from the final results, the final ones being C, O, Sn, Ba and Bi. Carbon is the major constituent element since the sample was placed on a carbon tape in order to be analyzed. The difference between the two sets of results is due to the area that was taken into focus, the second set being a good proof of elemental composition of the powder grains being, as already stated, in good accordance with the molarity of the materials used in the obtaining procedure.

Figure 3 presents the spectra for the analyzed materials. For all constituent elements there is an observable peak in the corresponding spectra. It can be seen in C and D spectra that peak for Chlorine and Sulfur are also present. These elements are remnants of the obtaining process, the quenching turning out to be insufficient for their removal.

From the microscopic point of view, the elemental composition of the obtained additives presents a good distribution among the samples. These results are in line with the desired materials composition, their behavior as additives in polymers will be studied further on.

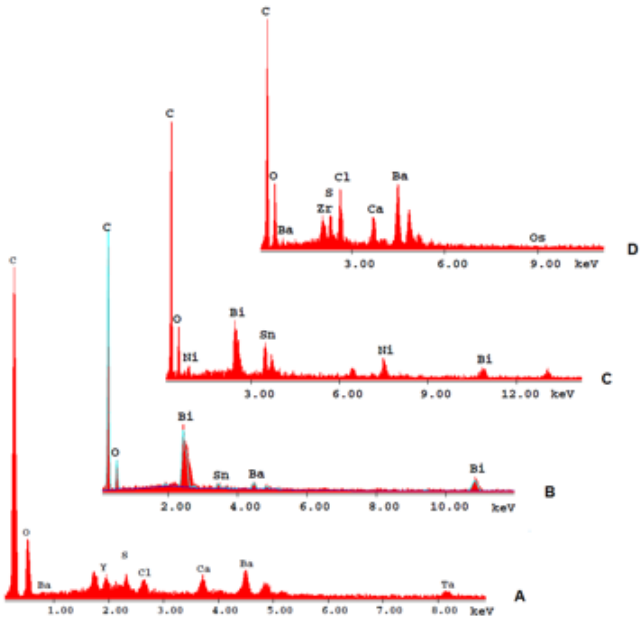

Fig. 3. Spectra from EDX analysis of powdery materials: A – $Y_{X1}Ta_{X2}Ba_{X3}Ca_{X4}O_{X5}$ powder; B – $Bi_{X1}Ba_{X2}Sn_{X3}Li_{X4}O_{X5}$ powder; C – $Sn_{X1}Bi_{X2}Ni_{X3}O_{X4}$ and D – $Os_{X1}Zr_{X2}Ba_{X3}Ca_{X4}O_{X5}$ powder

Raman scattering characterization of studied materials

All powders were analyzed using the Raman scattering technique and for each one, a spectrum was obtained. All spectra (fig. 4) were compared with the available BIO-RAD database and no clear result was obtained. This is due to a complex composition of the materials, which also could contain structures without correspondent in the utilized database. Future researches could also include X-ray diffraction analysis, in case any crystalline structures are formed in the obtaining process.

Despite the lack of clear chemical composition of the samples, the obtained results from the Raman analysis offers some clues regarding the similitudes between the studied materials. For example, the materials containing barium and calcium share a good deal of peaks (some exact values in cm^{-1} being made clearly visible on the graph), the curves for $Y_{X1}Ta_{X2}Ba_{X3}Ca_{X4}O_{X5}$ and $Os_{X1}Zr_{X2}Ba_{X3}Ca_{X4}O_{X5}$ powders are being overlapped from the beginning of the X axis until 1200 cm^{-1}. Also all the barium containing powders ($Bi_{X1}Ba_{X2}Sn_{X3}Li_{X4}O_{X5}$, $Y_{X1}Ta_{X2}Ba_{X3}Ca_{X4}O_{X5}$ and $Os_{X1}Zr_{X2}Ba_{X3}Ca_{X4}O_{X5}$ powders) are more or less overlapped starting from ~1700 cm^{-1} until the end of the X axis. These similitudes fit nicely in accordance with the results from the electrical conductivity tests, the abovementioned powders (the ones containing barium and calcium) sharing close values of this parameter, further on presented in this study.

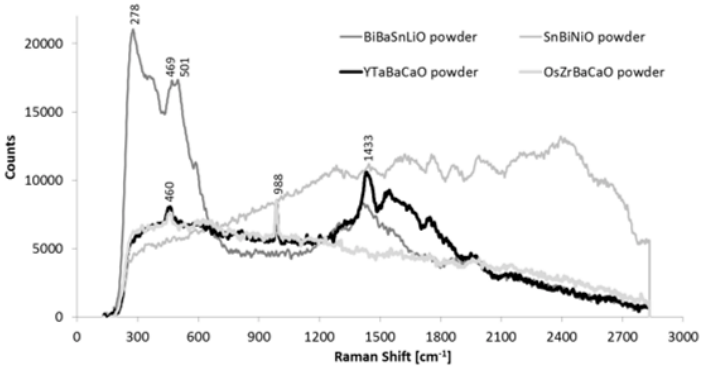

Fig. 4. Raman spectra obtained for the studied powdery materials: $Bi_{X1}Ba_{X2}Sn_{X3}Li_{X4}O_{X5}$; $Sn_{X1}Bi_{X2}Ni_{X3}O_{X4}$; $Y_{X1}Ta_{X2}Ba_{X3}Ca_{X4}O_{X5}$ and $Os_{X1}Zr_{X2}Ba_{X3}Ca_{X4}O_{X5}$ powders

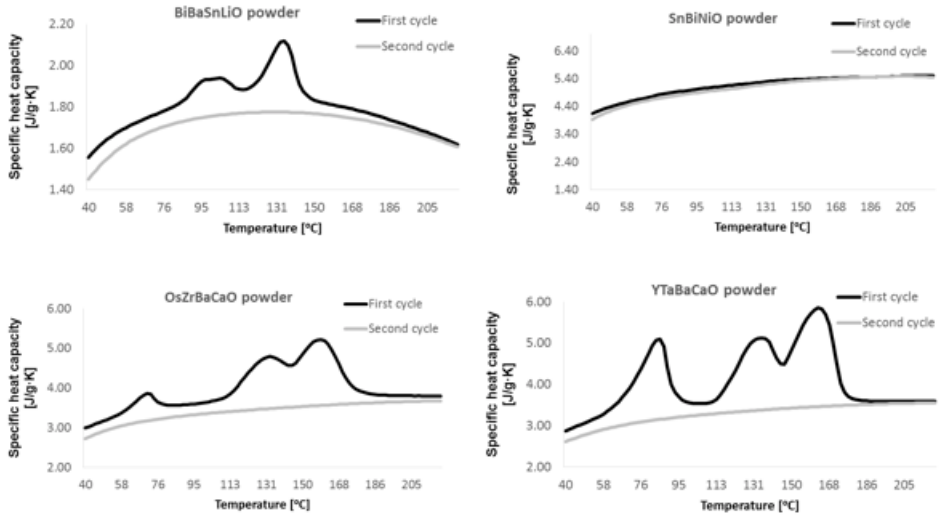

Fig. 5. Specific heat capacity evolution of each analyzed powders for first and second heat cycles during the differential scanning calorimetry analysis

Table 3

SPECIFIC HEAT CAPACITY VALUES FOR EACH ANALYZED MATERIAL ACCORDING TO FIRST AND SECOND HEATING CYCLES IN TWO TEMPERATURE INTERVALS (40-55 AND 80-100 °C)

	Specific heat capacity [J/g·K]							
	$Bi_{X1}Ba_{X2}Sn_{X3}Li_{X5}$		**$Sn_{X1}Bi_{X2}Ni_{X3}O_{X4}$**		**$Os_{X1}Zr_{X2}Ba_{X3}Ca_{X4}O_{X5}$**		**$Y_{X1}Ta_{X2}Ba_{X3}Ca_{X4}O_{X5}$**	
Temperature interval [°C]	**1st cycle**	**2nd cycle**	**1st cycle**	**2nd cycle**	**1st cycle**	**2nd cycle**	**1st cycle**	**2nd cycle**
40-55	1.63	1.53	4.33	4.17	3.14	2.87	3.03	2.75
80-100	1.87	1.74	4.98	4.85	3.59	3.30	4.29	3.18

Differential scanning calorimetry analysis of powders

For specific heat capacity calculation of the studied samples the DSC analysis consisted in two cycles of heating and cooling, the temperatures used being the before mentioned ones. For each cooling or heating cycle a curve was obtained. Figure 5 presents only the heating curves corresponding to each analyzed material.

All four graphs present similar trends for both heating curves obtained for each material, a striking difference between cycle 1 and cycle 2 curves corresponding to all materials except one ($Sn_{X1}Bi_{X2}Ni_{X3}O_{X4}$ powder) being the presence of some peaks for the cycle 1 curve. The presence of these peaks only for the cycle 1 curves is considered to be due to thermal degradation of some water that might have been reacted with the samples during their transfer from the quenching oven to the DSC analyzer. Another argument for this is the temperature used in the final step of obtaining the materials (800 °C) which was much higher compared to the ones corresponding to the peaks in the graphs and is thus excluding the possibility of compounds formation during the DSC analysis or the existing of organic substances. Taking into consideration the abovementioned facts, all three materials (with peaks on the first heating curve) will have to be kept some time at ~190 °C before being used as additives in polymers formation processes.

Regarding the specific heat capacity values for each material, valid are considered to be the ones obtained from the second cycle curve. Table 3 is presenting some mean values of this parameter for both heating cycles and for two temperature intervals. These two temperature intervals are considered representative for the future composite materials that might be obtained using the analyzed powders. The results show that $Bi_{X1}Ba_{X2}Sn_{X3}Li_{X4}O_{X5}$ powder has the lowest specific heat capacity between all four materials, which is a proof of a more efficient heat exchange of this material compared to the other ones, from this point of view this material being preferred for future utilization as additive.

Table 4

ELECTRICAL CONDUCTIVITY OF THE POWDERY SAMPLES, EXPRESSED IN S/m

Sample	**Electrical conductivity [S/m]**
$Bi_{X1}Ba_{X2}Sn_{X3}Li_{X4}O_{X5}$	$1.55 \cdot 10^{-4}$
$Sn_{X1}Bi_{X2}Ni_{X3}O_{X4}$	$3.08 \cdot 10^{-5}$
$Os_{X1}Zr_{X2}Ba_{X3}Ca_{X4}O_{X5}$	$1.13 \cdot 10^{-5}$
$Y_{X1}Ta_{X2}Ba_{X3}Ca_{X4}O_{X5}$	$1.30 \cdot 10^{-5}$

Determination of conductivity for powdery materials

The essential characteristic of the obtained materials was set to be a good conductivity, since their future utilization is conditioned by this property. Thus, the materials presented above are the ones with the highest conductivity.

The electrical conductivity for each studied material is presented in table 4. The best result was obtained for the powder containing lithium ($1.55 \cdot 10^{-4}$ S/m), while the samples containing Ca registered the smallest values, namely $1.13 \cdot 10^{-5}$ S/m and $1.30 \cdot 10^{-5}$ S/m respectively. According to the literature, these values are situated between the electrical conductivity of deionized water ($5.5 \cdot 10^{-6}$ S/m) [25] and drinking water ($5.00 \cdot 10^{-4}$ to $5.00 \cdot 10^{-2}$ S/m) [26]. These results are well below the conductivity of

graphene, namely $1.00 \cdot 10^8$ S/m, which is the highest that a material can deliver [27]. An inherent high conductivity for the obtained powders is of course one of the purposes of our research. The low values presented above were expected, since the tested materials were in powdery state. However, an increase of the electrical conductivity is planned to be further realized by subjecting the samples to different types and/or degrees of electromagnetic radiation and temperatures. The results of these experiments will be the focus of a future work.

Conclusions

One of the first steps in obtaining special properties polymers is to identify the additives that will give the desired properties. Sometimes, the material has to be first obtained, which is also the case of the present research. The main aims of this study were to obtain powders with nano-sized particles and good electrical conductivity. By using chemicals from Sigma Aldrich and a sol-gel method, twelve different powders were obtained, from which only four were taken into discussion in this paper.

Since the exact chemical composition of the materials is yet an unknown the powders were named as follow: $Bi_{X1}Ba_{X2}Sn_{X3}Li_{X4}O_{X5}$; $Sn_{X1}Bi_{X2}Ni_{X3}O_{X4}$; $Os_{X1}Zr_{X2}Ba_{X3}Ca_{X4}O_{X5}$ and $Y_{X1}Ta_{X2}Ba_{X3}Ca_{X4}O_{X5}$. All four materials were analyzed by SEM and proven to contain agglomerates of nanometer sized particles. These grains were studied by EDX and also proven to contain the elements and to some extent the stoichiometry of the salts used in their formation. Using the Raman scattering some similarities were observed between barium and calcium containing materials, similarities observed also after DSC and electrical resistance analyses.

All four presented materials are made of nano-sized particles and among the twelve obtained powders these ones present the highest electrical conductivity values. The future work will aim on characterizing these materials from the chemical/mineralogical point of view; particle size distribution; variation of electrical conductivity in different conditions (different electromagnetic irradiation and temperatures) and finally utilization as additives in obtaining special properties polymers.

Acknowledgements: The authors would like to acknowledge the financial contribution of the Project 12 P01 024 21 (C11) /31.08.2012 (code SMIS 50414).

References

1. SPITALSKY, Z., TASIS, D., PAPAGELIS, K., GALIOTIS, C., Prog. Polym. Sci., **35**, 2010, p. 357.
2. CHEN, J. K., LEI, J. T., ZHANG, M. H., BAI, S. L., Mech. Mater., **91**, 2015, p. 26.
3. WANG, Z., FANG, M., LI, H., WEN, Y., WANG, C., PU, Y., Compos. Sci. Technol., **117**, 2015, p. 410.
4. HUANG, E. Q., ZHAO, J., ZHA, J. W., ZHANG, L., LIAO, R. J., DANG, Z. M., J. Appl. Phys., **115**, 2014, 194102.
5. LI, K., WANG, H., XIANG, F., LIU, W., YANG, H., Appl. Phys. Lett., **95**, 2009, p. 202.
6. DANG, Z. M., YU, Y. F., XU, H. P., BAI, J., Compos. Sci. Technol., **68**, 2008, p. 171.
7. ZAK, A. K., GAN, W. C., MAJID, W. H. ABD., MAJID, D., VELAYUTHAM, T. S., Ceram. Int., **37**, 2011, p. 1653.
8. GAUTIER, B., WU, X., ALTAL, F., CHEN, S., GAO, J., Organic Electronics, **28**, 2016, p. 47.
9. MEIER, S. B., TORDERA, D., PERTEGÁS, A., ROLDÁN-CARMONA, C., ORTÍ, E., BOLINK, H. J., Materials Today, **17**, nr. 5, 2014, p. 217
10. BRANCHI, M., SGAMBETTERRA, M., PETTITI, I., PANERO, S., ASSUNTA NAVARRA, M., Int. J. Hydrogen Energy, **40**, 2015, p. 14757.
11. MOHAMMADI, G., JAHANSHAHI, M., RAHIMPOUR, A., Int. J. Hydrogen Energy, **38**, 2013, p. 9387.
12. SOTTO, A., BOROMAND, A., BALTA, S., DARVISHMANASH, S., KIM, J., VAN DER BRUGGEN, B., Desal. Water Treat., **34**, nr. 1-3, 2012, p. 179.
13. LI, X., LI, J., VAN DER BRUGGEN, B., SUN, X., SHEN, J., HANA, W., WANG, L., RSC Adv., **5**, 2015, p. 50711.
14. DUAN, L., ZHAO, X., WANG, Y., SHEN, H., GENG, W., ZHANG, F., J. Alloys Compd, **645**, 2015, p. 529.
15. MEHER, S. R., BIJU, K. P., JAIN, M. K., J. Sol-Gel Sci. Technol., **52**, 2009, p. 228.
16. AGARTAN, L., KAPUSUZ, D., PARK, J., OZTURK, A., Ceram. Int., **41**, 2015, p. 12788.
17. HSU, K. F., TSAY, S. Y., HWANG, B. J., J. Mater. Chem., **14**, 2004, p. 2690.
18. SANJAY KUMAR, D., ANANTHASIVAN, K., VENKATA KRISHNAN, R., AMIRTHAPANDIAN, S., DASGUPT, A., J. Nucl. Mater., **468**, 2016, p. 178.
19. ZHANG, L., The Ohio State University, 23 March 2004.
20. ZHUANG, Y., XU, Z., LI, F., LIAO, Z., LIU, W., J. Alloys Compd., **629**, 2015, p. 113.
21. FANG, P., XI, Z., LONG, W., LI, X., J. Alloys Compd, **657**, 2016, p. 273.
22. ISASI, J., PEREZ, M., CASTILLO, J. F., CORRECHER, V., ALDAMA, I., ARÉVALO, P., CARBAJO, M. C., Mater. Chem. Phys., **136**, 2012, p. 160.
23. ZANFIR, A. V., VOICU, G., JINGA, S. I., VASILE, E., IONITA, V., Ceram. Int., **42**, 2016, p. 1672.
24. BRIA, V., CIRCIUMARU, A., BIRSAN, I. G., Mat. Plast., **48**, no. 2, 2011, p. 189.
25. PASHLEY, R. M., RZECHOWICZ, M., PASHLEY, L. R., FRANCIS, M. J., J. Phys. Chem., B, 109 3: 1231–8.doi:10.1021/jp045975a, 2005.
26. *** https://en.wikipedia.org/wiki/Electrical_resistivity_and_conductivity, Retrieved on 2015-07-03.
27. *** newsdesk.umd.edu (2008-03-24). Retrieved on 2015-02-03.

Manuscript received: 27.05.2016